A pressure gauge based on gas density measurement from analysis of the thermal noise of an atomic force microscope cantilever

Dongjin Seo,[1] Mark R. Paul,[2] and William A. Ducker[1,a)]
[1]*Department of Chemical Engineering, Virginia Tech, Blacksburg, Virginia 24061, USA*
[2]*Department of Mechanical Engineering, Virginia Tech, Blacksburg, Virginia 24061, USA*

(Received 5 March 2012; accepted 28 April 2012; published online 15 May 2012)

We describe a gas-density gauge based on the analysis of the thermally-driven fluctuations of an atomic force microscope (AFM) cantilever. The fluctuations are modeled as a ring-down of a simple harmonic oscillator, which allows fitting of the resonance frequency and damping of the cantilever, which in turn yields the gas density. The pressure is obtained from the density using the known equation of state. In the range 10–220 kPa, the pressure readings from the cantilever gauge deviate by an average of only about 5% from pressure readings on a commercial gauge. The theoretical description we use to determine the pressure from the cantilever motion is based upon the continuum hypothesis, which sets a minimum pressure for our analysis. It is anticipated that the cantilever gauge could be extended to measure lower pressures given a molecular theoretical description. Alternatively, the gauge could be calibrated for use in the non-continuum range. Our measurement technique is similar to previous AFM cantilever measurements, but the analysis produces improved accuracy. [http://dx.doi.org/10.1063/1.4717678]

I. INTRODUCTION

The accurate measurement of pressure is essential in many areas of science and engineering. Many types of pressure gauges are available, using either mechanical or electrical mechanisms to sense the pressure; the preferred method depends on the range of gas pressure. One of the most common methods in the range 0.1–1000 Pa ($10^{-3} \sim 10$ torr) is the Pirahni gauge, which senses the thermal conductivity of the gas. At constant temperature, the thermal conductivity is proportional to the number density of gas molecules so the Pirahni gauge is essentially a gas density sensor.[1] The Pirahni gauge measures the resistance of a wire exposed to the gas, and the resistance decreases at lower temperatures. The wire is heated by an electrical current and cooled by heat transfer into the gas. Heat transfer into the gas is lower at lower pressure, so at lower pressure, the temperature increases and so does the resistance.[2]

Existing commercial gauges provide good performance for large volumes of gas, but there is a need for accurate pressure measurement in small volumes for micro- and nano-sized devices such as microelectromechanical systems.[3] Micron-sized structures, such as microfabricated cantilevers, have been used to study and measure a number of chemical, biological, and physical properties,[4,5] including pressure, P, which has been obtained from the quality factor, Q, and the resonance frequency of driven cantilevers in fluid. For example, Bianco *et al.*[6] examined driven microfabricated cantilevers, then related the quality factor and the resonance frequency to pressure using theories from Christian,[7] Bao *et al.*,[8] and Hosaka *et al.*[9] Bianco *et al.* showed that the quality factor is inversely proportional to pressure in the molecular region, and inversely proportional to the square root of pressure in the continuum region. Ekinci *et al.*[10] examined driven doubly clamped micron beams (micron bridges) and cantilevers. They also reported that the quality factor was inversely proportional to the square root of P in the continuum region and inversely proportional to P in the molecular region. Other researchers[11,12] determined the pressure using the theory by Christian[7] and Hosaka *et al.*[9] They also reported that their results were in good agreement with the theories, concluding that $Q \sim 1/P^{1/2}$ in the continuum regime and $Q \sim 1/P$ in the molecular regime.

Instead of relating pressure to the quality factor and resonant frequency using theory, Mortet *et al.*[13] calibrated a specific piezoelectric bimorph microcantilever by measuring the resonant frequency change as a function of pressure and temperature, i.e., pressure was determined empirically.

To be practical, a gauge should be able to measure the pressure over some defined range with a specified error, and preferably the pressure should be predicted from Q and the resonance frequency using theory. At this point there are several good measurements and theories, but what is lacking is an AFM cantilever pressure gauge that has a specified agreement with theory over a useful and specified range of pressures. In this paper, we describe a method that is based on the theory of Paul and Cross[14] that can be used to measure the gas pressure in the range 10–225 kPa with an error that is 5% on average.

II. THEORY

There have been many analytical investigations of the dynamics of small objects such as cylinders and cantilevers immersed in a viscous fluid.[15–19] Of particular relevance to our approach is the work of Sader,[19] which provided a detailed analytical description of the dynamics of oscillating cantilevers immersed in a viscous fluid for the case of long

a)Author to whom correspondence should be addressed. Electronic mail: wducker@vt.edu.

and thin cantilevers where the cantilever length is much larger than its width. Paul and Cross[14] then developed a theoretical description of the stochastic behavior of a cantilever immersed in a viscous fluid that is driven by Brownian motion. We have used this theoretical description in our analysis here. In the following, we present only the essential details of the theoretical background (for more details see Ref. 20). The frequency dependence of the Brownian force is included via the fluctuation-dissipation theorem which states that the thermal fluctuations of a system at equilibrium are directly related to the dissipation in the system. Using linear response theory it has been shown that the deterministic response of the cantilever to a small perturbation away from equilibrium can be used to find the stochastic dynamics. Using deterministic numerical simulations for the cantilever ring-down allows one to quantify the stochastic dynamics of the cantilever for the precise conditions of experiment. In the limit of long and slender cantilevers, as is the case in our experimental measurements presented here, it is possible to develop an analytical description of the stochastic cantilever dynamics. Specifically, the auto-correlation of equilibrium fluctuations of the cantilever displacement can be found from the deterministic ring down of the cantilever to the removal of step force. This can be represented as

$$\langle x(0)x(t)\rangle = \frac{k_B T}{F} X(t), \tag{1}$$

where x is the stochastic deflection of the cantilever tip, t is the time, k_B is the Boltzmann constant, T is the absolute temperature, F is the magnitude of force applied to the cantilever tip at some time in the distant past that is removed at time zero, $\langle\ \rangle$ denotes an equilibrium ensemble average, and $X(t)$ denotes the deterministic displacement of the cantilever tip due to the removal of the force. Equation (1) relates an easily measurable quantity, the autocorrelation of the thermal motion, to a deterministic and more easily modeled quantity, the displacement of a cantilever.

If the deterministic ring-down of the cantilever is modeled as a simple harmonic oscillator as with Paul *et al.*,[20] the time-dependent displacement of the cantilever is given by

$$X(t) = \frac{F}{k} e^{-\omega_f t/2Q}\left(\cos(\omega' t) + \frac{\omega_f}{2Q\omega'} sin(\omega' t)\right), \tag{2}$$

where

$$\omega' = \omega_f \sqrt{1 - \frac{1}{4Q^2}}, \tag{3}$$

where k is the equivalent spring constant of the cantilever and ω_f is the resonant frequency of the cantilever when immersed in fluid which we determine as the frequency at the maximum amplitude of power spectral density. The quality factor can then be related to the mass density of the fluid, ρ, by combining Eqs. (25), (29), and (41) in Paul *et al.*[20] to yield

$$\frac{\alpha\pi w^2 L\omega_f^2}{4k}\Gamma''(R_\omega) = \frac{1}{Q}, \tag{4}$$

where w is the width of the cantilever, L is the cantilever length, $\alpha = 0.243$ is a parameter accounting for our representation of the cantilever as a lumped mass, and R_ω is the nondimensional frequency parameter.

$$R_\omega = \frac{\rho\omega_f w^2}{4\eta}, \tag{5}$$

where η is the dynamic viscosity of the surrounding fluid which depends on temperature but not on pressure in general. Γ'' is the imaginary part of the complex hydrodynamic function,

$$\Gamma(\omega_f) = 1 + \frac{4iK_1(-i\sqrt{iR_\omega})}{\sqrt{iR_\omega}K_0(-i\sqrt{iR_\omega})}, \tag{6}$$

where K_1 and K_0 are Bessel functions.

Equation (4) can be used to obtain either the density or the viscosity from the quality factor and the resonant frequency. Here, we use the known viscosity (which is almost independent of pressure, but depends on temperature) to obtain the gas density. Pressure can be calculated from the density with an appropriate equation of state. At the pressures considered in this paper, the compressibility of air and nitrogen is very close to one so they obey the ideal gas equation, $P = (\rho/m_m)RT$, where m_m is the molar mass of the gas, and R is the gas constant. Substitution of the ideal gas equation into Eq. (4) yields

$$\frac{\alpha\pi w^2 L m_m \omega_f^2}{4k}\frac{P}{RT}\Gamma''\left(\frac{P}{RT}\frac{m_m\omega_f w^2}{4\eta}\right) = \frac{1}{Q}, \tag{7}$$

which we use here to obtain the pressure from the quality factor.

III. EXPERIMENTS

AFM cantilevers were purchased from Bruker Corporation (Model No. OCR8-W).[21] Two nominally identical cantilevers (B and C) and one different cantilever (A) were used (see Table I). The unclamped end of the cantilevers is tapered. The spring constants, k, were measured from the thermally stimulated changes in endslope (the Hutter method)[22] using the light-lever technique in an Asylum instruments MFP-3D, then the length and width were measured using an optical microscope. Equations (4) and (7) do not require knowledge of the cantilever thickness.

The resonance properties of each cantilever were measured in a cylindrical glass jar with a screw-top lid. The endslope of the cantilever was measured with a homebuilt light lever sensor consisting of a laser (681 nm, Schäfter + Kirchhoff GmbH) and a split photodiode (Phresh Photonics) connected via an A/D card (PCI-6110, National Instruments) to a computer. Temperature was recorded with a thermometer (TH-3, AMPROBE).

TABLE I. Measured spring constants and dimensions of cantilevers.

Designation	A	B	C
k, pN/nm	102	46	42
Length, μm	202	202	198
Width, μm	37	18	18

The pressure was reduced below atmospheric pressure with a vacuum pump, and increased with pure dry nitrogen. The pressure inside the glass jar was measured with a DPG25V gauge (SUPCO) for $P > 7$ kPa with a manufacturer's stated error of $\pm 0.5\%$ of the reading, and Digivac 276 (Digivac Co.) for $P < 7$ kPa with varying errors listed on their product information page.[23] Digivac 276 senses the electric properties of a thermocouple with varying pressure, while DPG25V is a differential gauge. In our implementation, various commercial pressure gauges did not agree with each other (within the stated error) so the actual errors in gas measurement in our implementation were greater than under the manufacturer's conditions. This was particularly a problem for 1.5 kPa $> P >$ 12 kPa. We limit our conclusions to pressures greater than 10 kPa because of uncertainty in the known pressure for comparison to our measurement from the cantilever-gauge.

After the desired pressures were reached, a time series of the cantilever deflection was collected for 15 s (cantilevers A and B) or 5 s (cantilever C) with 1 μs intervals between periods of data collection. For cantilevers A and B, the 15 million data points were divided into 500 sequential windows of 30 000 data points. The data in each window was detrended by subtraction of the best linear fit and was then processed using a fast Fourier transform. The transformed data was multiplied by its complex conjugate to provide the power spectral density for one window. The average power spectral density was computed by averaging the spectrum from all 500 windows. The auto-correlation of the equilibrium fluctuations was then determined by computing the inverse fast Fourier transform of the averaged power spectral density. For cantilever C, 5 million data points were divided into 500 sequential windows of 10 000 data points.

Our deflection measurements were in arbitrary units, which we then normalized such that the auto-correlation at zero time lag was unity. This is equivalent to setting the area under the power spectral density to $k_B T/k$ as was done to calibrate the spring constant. As shown in Eq. (1) the auto-correlation of the equilibrium fluctuations are directly related to the deterministic ring-down of a simple harmonic oscillator which is given by Eq. (2). We obtained values for Q and ω_f by fitting our experimental results with Eq. (2). The cantilever-gauge pressure is the gas pressure calculated using Eq. (7). The analytical theory we are using is for a cantilever with a constant value of the width for the entire length of the cantilever. However, the cantilevers used in the experiments had a slight taper in width near the unclamped end, so there is no unique width. Since our cantilevers had no unique width we measured an "effective width" at atmospheric pressure (where the pressure was known) and we have used this constant width for all the data sets to calculate pressures with Eq. (7). For example, the effective width of the cantilever B was 14 μm, rather than the nominal width of the cantilevers, 18 μm. The significant discrepancy between the fitted width and the measured nominal width suggests that this parameter may also be accounting for effects other than the width of the cantilevers. Note that the molar mass of the gas can be included in this effective width, if unknown.

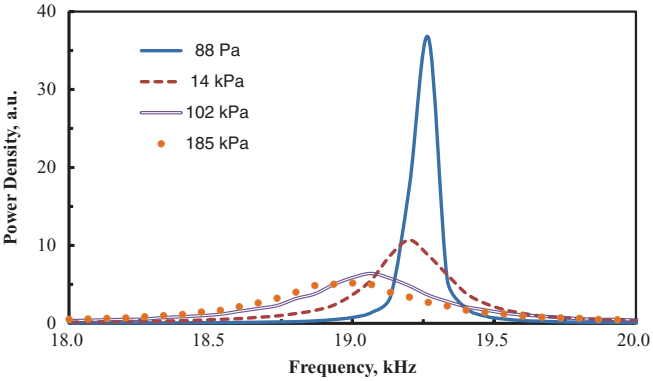

FIG. 1. Power spectral density for cantilever B at 4 different pressures. At higher pressure, the fundamental resonance shifted to lower frequency and the width of the peak was broader.

IV. RESULTS

For cantilever A, 28 data sets were obtained for the power spectral density and auto-correlation. The first set was measured at the atmospheric pressure of the day, recorded as 102 kPa, which was used to calculate the effective width of the cantilever. For cantilever B, 19 data sets were collected along with the data set at atmospheric pressure. For cantilever C, 37 data sets were measured. Combining the experiments from all three cantilevers the pressure varies from 33 Pa to 225 kPa. The temperature in the lab varied between 292 K and 297 K. Examples of the power spectral density are shown in Figure 1 for a variety of gas pressures. The spectra in Figure 1 (and other spectra not shown here) were in accordance with the qualitative expectation that an increase in pressure led to both a shift to lower resonance frequency and a broadening of the resonance peak (lower Q).

The pressure from Eq. (7), using the fitted values of Q and ω_f, is shown as a function of the pressure measured by the commercial gauge in Figure 2. Figure 2(a) shows the comparison over all pressures for all three cantilevers on a log scale, whereas Figure 2(b) shows a subset of data where the pressure exceeds 10 kPa, on a linear scale.

Clearly the pressure obtained from the cantilever agrees well with the pressure from the differential gauge in the range 10–225 kPa. The percentage deviation between the two measured pressures is shown in Figure 3; on average there is only a 5% deviation between the two gauges.

Figure 2(a) shows the pressure predicted by Eq. (7) systematically deviates from the thermocouple gauge, Digivac 276, at pressures below 10 kPa for cantilevers B and C. This is expected because we have used a continuum theory of the gas. The transition between continuum and molecular behavior is characterized by the Knudsen number, Kn = mean free path/characteristic length. In this case, the characteristic length is the effective width of the cantilevers $\approx$14 μm for cantilever B and C. Typically, the continuum regime applies to Kn < 0.1.[6,24] For air, 10 kPa is equivalent to Kn $\approx$0.07, so the deviation occurs approximately at the expected pressure. Cantilever A is wider, with an effective width of 35 μm, and therefore the pressure is lower before the mean free path reaches one tenth of the cantilever width (Kn = 0.1). This is consistent with observation: Figure 2(a) shows that pressure

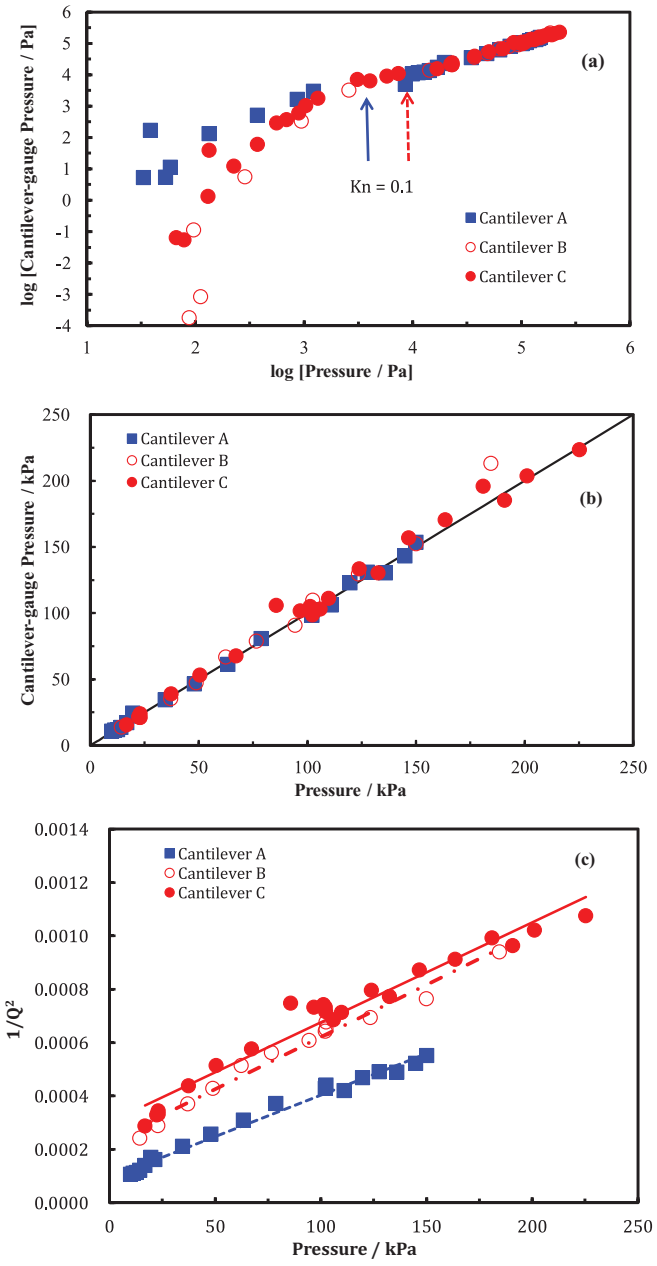

FIG. 2. Cantilever-gauge pressure as a function of the measured pressure. Cantilever-gauge pressure is the pressure calculated with Eq. (7). (a) All data is shown using a log scale. The arrows point to the pressure where Kn = 0.1 (solid blue for cantilever A, dashed red for B and C), and thus to the approximate limit of applicability of equations assuming continuum behavior. (b) $P > 10$ kPa on a linear scale. The solid black line shows equal pressure on the commercial and cantilever gauges. (c) Comparison of our experiments with the trend $Q \sim 1/P^{1/2}$ as suggested in the literature.[6,9–12] The dashed blue line is the linear trend for cantilever A, the red dash-dot line is the linear trend for cantilever B, and the solid red line is for cantilever C.

measurements from the wider cantilever A using Eq. (7) have better agreement with the commercial gauge at lower pressure than the narrower B and C cantilevers.

For comparison to previous work (see Sec. I), we have also examined how well our data agrees with the relation, $P \propto 1/Q^2$. Figure 2(c) shows the fitted values of $1/Q^2$ plotted as a function of measured differential gauge pressure for data in the range 10–225 kPa along with a best fit line for each cantilever. The mean deviation of the points from the line is 15%, which is worse than the deviation of 5% using the analysis from Paul *et al.* (see Sec. II) but still useful for more approximate work. Note that simply using $P \propto 1/Q^2$ to determine pressure also requires fitting a line to data points at several pressures (i.e., a calibration set), whereas our method requires only calibration of an effective width at atmospheric pressure. Also, the errors in our method (see Fig. 3) are roughly distributed about zero whereas the $1/Q^2$ method shows a trend to lower $1/Q^2$ at higher pressure and higher $1/Q^2$ at lower pressure.

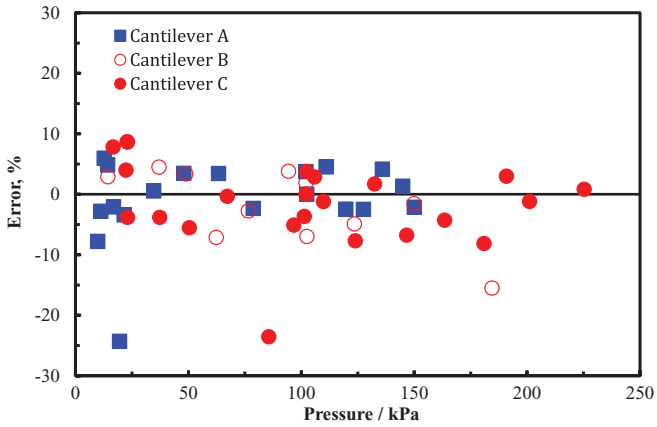

FIG. 3. Percentage error of cantilever-gauge pressure from the commercial-gauge pressure in the range 10–225 kPa. The error is calculated as 1-(cantilever-gauge pressure/commercial-gauge pressure). Except for three data points, the errors are within 10%. The mean error is 5%.

V. DISCUSSION: EFFECT OF TEMPERATURE AND HUMIDITY

Equation (7) explicitly depends on the temperature, but the main effect of temperature is through the effect on the viscosity. In the analysis described here, we measured the temperature, and used the measured temperature in Eq. (7), but it is interesting to also examine the sensitivity of the pressure calculated from Eq. (7) to changes in temperature, for use of the gauge without a thermometer. For a measurement at 19 °C, an input of 18 °C in Eq. (7), yields a pressure that is 1% greater; an input of 25 °C, yields a pressure that is 2% lower. Thus, the use of an approximate guess of the temperature results in only small errors in the measured pressure.

Humid environments can potentially affect the operation and interpretation of the gauge in two ways; by forming a wetting film on the cantilever and by affecting the gas properties. Cantilevers typically have a finite water contact angle, so adsorbed water films will be thin, even compared to the thickness of the cantilever (< 1 μm). The combination of a very hydrophilic (clean) cantilever and variable humidity above 80% at high pressure (~1 atm) should be avoided so as to avoid errors due to changing mass of the cantilever after calibration. Humidity also affects the density and viscosity of the gas, but these effects can be included explicitly through the use of tabulated data for the density and viscosity of humid air (e.g., in Ref. 25). The effects of an unknown humidity on the measurement can be estimated from tabulated data. At 1 atm and room temperature, the partial pressure of saturated

water vapor is only about 2% of the total pressure, and thus neglect of a humidity change from 0%–100% only affects the measured density and viscosity by about 1% and 2%, respectively, which would cause a 6% error in the measured pressure if ignored. The partial pressure of water vapor increases with temperature, so the effect of humidity on viscosity and density should not be ignored nearer to the boiling point of water. So, in summary, the effects of both humidity and temperature are simply included if the humidity and temperature are measured. If they are not, this neglect causes only a minor effect on the measured pressure, except at high temperature, and possibly for a cantilever that is completely wet by water.

VI. CONCLUSION AND OUTLOOK

The pressure of gases near one atmosphere was obtained from measurements of the auto-correlation of equilibrium fluctuations in AFM cantilever displacement. In the pressure range 10–225 kPa, the cantilever pressure gauge deviated by an average of 5% from values measured by a commercial differential gauge. At lower pressure, where the Knudsen number is greater than 0.1 and the theory is not expected to be valid, our pressure measurements were systematically lower than those from other gauges. The deviation of the cantilever gauge at low pressure was smaller when a wider cantilever was used (i.e., there was a lower Knudsen number at a given pressure). The quality factor and resonant frequency are still functions of pressure below 10 kPa, so the range of the pressure gauge could be extended to lower pressures using either a calibration curve (e.g., Figure 2(a)) or a theoretical description applicable at lower pressures.

The largest dimension of the cantilever is 200 μm, so the detector takes up a very small space in the gas. This device should be useful in microscale applications such as lab-on-a-chip and microflow applications. It may also find application in aeronautical applications where many sensors could be added in close proximity with little weight gain or interference with the flow. The sensor can be used to measure pressures above and below atmospheric pressure.

ACKNOWLEDGMENTS

The work described in this paper was funded by the National Science Foundation via Award No. CBET-0959228 and by Virginia Tech. The authors acknowledge useful discussions with John Walz, Brian Robbins, and Milad Radiom.

[1] A. Ellett and R. M. Zabel, Phys. Rev. **37**, 1102 (1931).
[2] J. F. O'Hanlon, *A User's Guide to Vacuum Technology*, 3rd ed. (Wiley, Hoboken, 2003), p. 89.
[3] W. P. Eaton and J. H. Smith, Smart Mater. Struct. **6**, 530 (1997).
[4] F. G. Barth, J. A. C. Humphrey, and T. W. Secom, *Sensors and Sensing in Biology and Engineering* (Springer-Verlag, New York, 2003), pp. 338–341.
[5] A. Raman, J. Melcher, and R. Tung, Nanotoday **3**, 20 (2008).
[6] S. Bianco, M. Cocuzza, S. Ferrero, E. Giuri, G. Piacenza, C. F. Pirri, A. Ricci, L. Scaltrito, D. Bich, A. Merialdo, P. Schina, and R. Correale, J. Vac. Sci. Technol. **24**, 1803 (2006).
[7] R. G. Christian, Vacuum **16**, 175 (1966).
[8] M. Bao, H. Yang, H. Yin, and Y. Sun, J. Micromech. Microeng. **12**, 341 (2002).
[9] H. Hosaka, K. Itao, and S. Kuroda, Sens. Actuators, A **49**, 87 (1995).
[10] K. L. Ekinci, V. Yakhot, S. Rajauria, C. Colosqui, and D. M. Karabacak, Lab Chip **10**, 3013 (2010).
[11] J. Lübbe, H. Schnieder, and M. Reichling, e-J. Surf. Sci. Nanotech. **9**, 30 (2011).
[12] G. Keskar, B Elliott, J Gaillard, M. J. Skove, and A. M. Rao, Sens Actuators, A **147**, 203 (2008).
[13] V. Mortet, R. Petersen, K. Haenen, and M. D'Olieslaeger, Appl. Phys. Lett. **88**, 133511 (2006).
[14] M. R. Paul and M. C. Cross, Phys. Rev. Lett. **92**, 235501 (2004).
[15] H.-J. Butt and M. Jaschke, Nanotechnology **6**, 1 (1995).
[16] E. O. Tuck, J. Eng. Math. **3**, 29 (1969).
[17] L. Rosenhead, *Laminar Boundary Layers* (Oxford University Press, Oxford, 1963).
[18] R. J. Clarke, O. E. Jensen, J. Billingham, A. P. Pearson, and P. M. Williams, Phys. Rev. Lett. **96**, 050801 (2006).
[19] J. E. Sader, J. Appl. Phys. **84**, 1 (1998).
[20] M. R. Paul, M. T. Clark, and M. C. Cross, Nanotechnology **17**, 4502 (2006).
[21] See http://www.brukerafmprobes.com/Product.aspx?ProductID=3378 for more information about the cantilevers.
[22] J. L. Hutter and J. Bechhoefer, Rev. Sci. Instrum. **64**, 1868 (1993).
[23] See http://www.digivac.com/get-educated/digivac-accuracy.html for more information about Digivac 276.
[24] S. Kakaç, L. L. Vasiliev, Y. Bayazitoglu, and Y. Yener, *Microscale Heat Transfer: Fundamentals and Applications* (Springer, Norwell, 2004), p. 3.
[25] P. T. Tsilingiris, Energy Convers. Manage **49**, 1098 (2008).